Theoretical Analysis of Adaptive Load Balancing Ad Hoc Routing Inspired by True Slime Mold

Hiroshi Katada*, Taku Yamazaki†, Takumi Miyoshi†,*
*Graduate School of Engineering and Science, Shibaura Institute of Technology
307 Fukasaku, Minuma-ku, Saitama-shi, Saitama, 337–8570 Japan
†College of Systems Engineering and Science, Shibaura Institute of Technology
307 Fukasaku, Minuma-ku, Saitama-shi, Saitama, 337–8570 Japan
Email: {mf18024,taku,miyoshi}@shibaura-it.ac.jp

***Abstract*—Biomimetics, which are imitation models based on body structures and behavior of living organisms to solve complex problems, have been studied in various fields. In distributed network fields such as ad hoc networks and wireless sensor networks, behavior of variety of true slime molds, which can construct multipath flow networks based on the amount of body, have been studied. Ad hoc networks only consist of mobile terminals (nodes) that can relay packets along an established route. However, link relations and available bandwidth of the nodes dynamically change due to the node mobility. Thus, practical use of ad hoc networks still remains an issue because it is difficult to establish stable routes under such environments. This study aims to propose an adaptive load balancing routing that adaptively diversifies the transmission paths based on the available bandwidth, residual battery, and the transmission data size by applying a mathematical model of slime mold routing, known as physarum solver. We confirm the effectiveness of its adaptive behavior under dynamic environments using computer simulations.**

***Index Terms*—Ad hoc network, Adaptive ad hoc routing, Biomimetics, True slime mold, Physarum solver**

I. Introduction

Life forms change and optimize their structures and behavioral patterns during evolutions. Recently, biomimetic technologies that design artifacts that inspired from their abilities and the structures have been studied. Major examples of biomimetic technologies include swimsuits inspired by the skin structure of sharks, and nylon fiber inspired by the fiber structure of cotton. In network research fields, various bio-inspired mechanisms, such as the multiple route optimization inspired by the feeding behavior of physarum [1], a shortest-path route optimization inspired from the feeding behavior of ants [2], and a synchronization mechanism inspired by synchronous behavior of fireflies, have also been studied [3]. The nature of *Physarum Polycephalum*, which is a variety of physarum, has been expected to be applied to a routing protocol. Note that we simply call *Physarum Polycephalum* physarum below. As a nature of the feeding process of physarum, it has been confirmed that physarum creates a tube for nutritional transport, utilizes its own body and connects foods using the tube when it finds multiple baits at different places. It also has been confirmed that the number of constructed paths varies depending on the amount of liquid constituting physarum. Therefore, physarum can optimize the trade-off between the efficiency and stability of nutritional transport paths, and thus the nature of physarum can be applied to a relay node selection in wireless multi-hop networks. As an application of the above nature, an ad hoc network that consists only of mobile wireless terminals (nodes), without relying on a base station, can be taken for instance [4]. The ad hoc network has exceptional use in an area where a base station cannot be placed or has been destroyed due to disaster. In ad hoc networks, nodes can communicate with each other by relaying packets called multi-hop communication when relay nodes exist, even if they are located out of communication range. However, due to factors such as node mobility, running out of battery, and radio interference, dynamic topology changes and network stability degradations may occur. One solution includes the use of a multipath routing protocol that can alleviate the impact of the dynamic changes by simultaneously using multiple paths.

In this study, we propose a multipath ad hoc routing method by applying a mathematical model inspired by the path finding ability in the nature of physarum called the physarum solver (PS) [5]. By applying PS, the proposed method constructs multiple paths and adaptively allocates the bandwidth to them based on the transmission data size, the available bandwidth of each link, and the residual battery of each node.

II. Related Work

A. Overview of Physarum-Inspired Path Finding Approach

Physarum consists of a stretchable tube and viscous liquid flowing through it. The tube is a path connecting multiple baits, and becomes thinner or thicker in response to the fluctuation in the flow rate. In addition, the tube has an upper limit to the thickness. Figure 1 shows a route construction example of physarum in a maze. First, physarum spreads its tube over the entire maze. Next, it selects paths where physarum finds food. Then, the tube gradually becomes thinner as the flow rate of the liquid decreases, when the

path is relatively longer than other paths. In addition, since flow does not occur in a blind tube, the tube degenerates relatively quickly. Therefore, physarum prioritizes shorter and continuous paths, and the number of remaining paths varies based on the total amount of liquid constituting physarum. In addition to the above properties, physarum moves away from sources of light (negative phototaxis), and therefore the tube becomes thinner at the segment exposed to light. If the path is disrupted by an external factor, physarum takes a detour path to reallocate the flow of the disrupted path to other paths to avoid path disruption of connectivity between the baits. Therefore, physarum can adjust the efficiency and stability of nutritional transport paths.

An experiment [6], which observed the behavior of physarum on a railway network, has been conducted. The experiment prepares an agar medium to imitate the railway network in the Kanto Region, and places bait at positions that correspond with major cities in the region. Then, physarum is placed in the position that corresponds with Tokyo, and the behavior of physarum has been observed. In the experiment, the light quantity is adjusted according to the elevation and position of the river to imitate the topography of the Kanto region. In the experimental results, physarum spreads in approximately a half day, and it becomes clear that the paths similar to the current railway network are constructed among baits. This result has revealed that the transport efficiency and stability of transport paths designed by humans and physarum are similar.

B. Physarum Solver

Physarum solver (PS) [5] is a mathematical model, which focuses on feeding behavior of physarum when physarum constructs a route between baits. PS calculates the flow rate of each tube based on the total amount of liquid in physarum, and length, thickness, and pressure loss of each tube. In the initial state, PS calculates the pressure loss in each tube based on the total amount of liquid, length, and thickness of the tube. Thereafter, the flow rate of each tube is temporarily determined in accordance with the pressure loss of the tube, and then the flow rate of the tube changes as the thickness varies. By iterating such process, the flow rate and thickness of the tube converge to an appropriate value, and finally the tubes remain based on the total amount of liquid. Furthermore, by setting parameters of phototaxis, it is possible to control the thickness of a tube without depending on the flow rate.

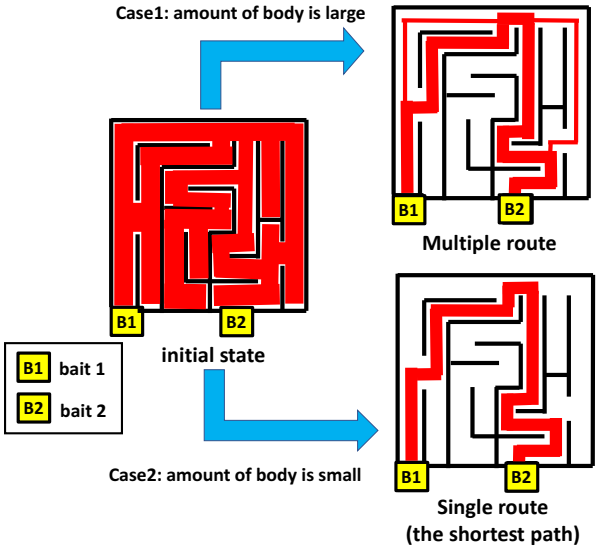

Fig. 1. Behavior of slime mold in the maze.

The operation procedure of PS when baits are placed in two places is shown below. Here, PS deals with tubes that have branch points i and j as both ends.

1) PS calculates the pressure loss of a tube between i and j from the flow rate of a tube, calculated by Eq. (1), and flow conservation law of a tube, calculated by Eq. (2).

$$Q_{ij}(t) = \frac{D_{ij}(t)}{L_{ij}}(p_i(t) - p_j(t)) \quad (1)$$

$$\sum_i Q_{ij} = \begin{cases} -Q_{\text{all}} & (j = \text{bait1}) \\ Q_{\text{all}} & (j = \text{bait2}) \\ 0 & (\text{otherwise}) \end{cases} \quad (2)$$

Where Q_{all} is the total amount of liquid; $D_{ij}(t)$ and L_{ij} are the thickness and length of a tube, respectively; $p_i(t) - p_j(t)$ is the pressure loss of a tube.

2) By substituting the derived pressure loss into Eq. (1), the flow rate of each tube $Q_{ij}(t)$ is temporarily determined, and thereby a shorter and thicker tube allows a larger flow rate. However, due to pressure loss in the blind tube, the flow rate also becomes small.
3) By substituting the flow rate of each tube in Eq. (3), PS updates the tube thickness.

$$D_{ij}(t + \delta t) = D_{ij}(t) + \delta t\{f(|Q_{ij}(t)|) - aD_{ij}(t)\} \quad (3)$$

$$\text{Here, } f(|Q_{ij}(t)|) = \frac{|Q_{ij}(t)|^\mu}{1 + |Q_{ij}(t)|^\mu}, \quad \mu > 1.0$$

a is a parameter expressing the extent of phototaxis and it controls the degeneration speed of the tube. When the flow rate is large or small, the variations in the thickness of the tube decrease since it changes based on a sigmoid curve. μ is a gradient of the sigmoid function. It is the convergence speed of the thickness of the tube.
4) PS reenters the updated tube thickness into Eq. (1).

By iterating the above procedure, PS converges the route between baits.

As described above, PS operates by treating the maze as a flow network. Therefore, it is possible to use PS as a solution for routing in computer networks and transportation networks.

Car navigation has been proposed as one application of PS [7]. In this method, the system determines a route on the interstate highway from Seattle to Houston in the United States based on PS. PS derives a single route with the shortest mileage, when there is no trouble in the transportation network. When routes are congested, PS obtains the route with the shortest time by changing the value of a according to the

traffic volume. Moreover, if an accident takes place in the middle of the route, PS obtains the optimum detour route to avoid the road where the accident has taken place.

C. Physarum-based Routing Scheme

A Physarum-based routing scheme (P-bRS) has been proposed that applies PS to routing in wireless sensor networks (WSN) [8]. The network model of P-bRS assumes multi-hop WSN consists of static sensor nodes and a single mobile sink node, which are uniformly arranged in a two-dimensional space. The network model also assumes that each sensor node can obtain the position information of all sensor nodes and the residual battery of the sensor nodes. The sink node broadcasts its current position periodically to the surrounding sensor nodes while moving along a specific route.

In P-bRS, each parameter of PS is redefined to apply PS to WSN. Eq. (1) and Eq. (3) are changed to Eq. (4) and Eq. (6), respectively.

$$\begin{aligned} Q_{ij}(t) &= \frac{D_{ij}(t)}{L_{ij}}(p_i(t) - p_j(t)) \\ &= \frac{k\mathrm{ER}_j(t) + (1-k)\cos\theta_{jid}}{L_{ij}} \\ &= \frac{P_{ij}(t)}{L_{ij}} \end{aligned} \tag{4}$$

$$\theta_{jid} = \arccos\frac{L_{ij}^2 + L_{jd}^2 - L^2 cd}{2L_{ij}L_{id}} \tag{5}$$

$$P_{ij}(t+\delta t) = P_{ij}(t) + \delta t\{(Q_{ij}(t))^{\mu} - P_{ij}(t)\} \tag{6}$$

Where $Q_{ij}(t)$ is virtual data packet size between node i to j; L_{ij} is the Euclidean distance of node i to j; ER_j is the residual battery of node j; θ_{jid} is the angle of deviation that is derived from the cosine formula, and its range is $[-\pi/2 \leq \theta_{ijd} \leq \pi/2]$. Figure 2 shows an example of next-hop selection in P-bRS. As shown in the figure, nodes closer to the sink node have a smaller angle of deflection. $D_{ij}(t)$ which is defined as the link quality is omitted in Eq. (4) because the model assumes that $D_{ij}(t)$ is always constant. The coefficient k is used to adjust the weight of the residual battery and the angle of deviation. Therefore, P-bRS constructs a route based on both the residual battery and the angle of deviation to replace the pressure loss in PS.

An operation procedure of P-bRS in the case of transmitting data from a sensor node i to a sink node d is shown below. When a data transmission request occurs, the sensor node i divides its communication range into a semicircle N_i^N, which is closer to the sink node, and a semicircle N_i^F, which is further from the sink node, based on the position information received from the sink node. Thereafter, node i calculates $P_{ij}(t)$ for node j that belongs to N_i^N using Eq. (4)–Eq. (6). Here, node i gives an order j_x, which is arranged by $P_{ij}(t)$ in descending order. Node i selects the node j_0 as a relay node and transmits a control packet to the node j_0. The node j_0 transmits the acknowledgement packet (ACK) to the node i after receiving the control packet. Then, if the node j_0 satisfies $N_{j_0}^N = \phi$, it does not transmit ACK. If node i has not received ACK from node j_0 after a certain period, node i selects the relay node j_x of the smallest x that satisfies $|\theta_{j_0id} - \theta_{j_xid}| \geq \pi/2$ and $N_{j_x}^N \neq \phi$, and transmits a control packet. If there does not exist node j_x, which satisfies these conditions, node i calculates $P_{ik}(t)$ for node k, which belongs to N_i^F. Here, node i gives an order k_y to the node k, which is arranged by $P_{ij}(t)$ in ascending order. Node i selects a relay node k_y, as in case of selection of node j_x, and retransmits the control packet to k_y. Therefore, P-bRS constructs a route to avoid the node in low density areas, thus it prevents an increase in the transmission delay. Node i initiates data transmission after receiving the ACK from the node j_x or k_y to finish its routing process. By iterating the above process until the data reaches the sink node, P-bRS constructs a route based on the Euclidean distance to the sink node, angle of deviation, and residual battery, while avoiding the low node density area.

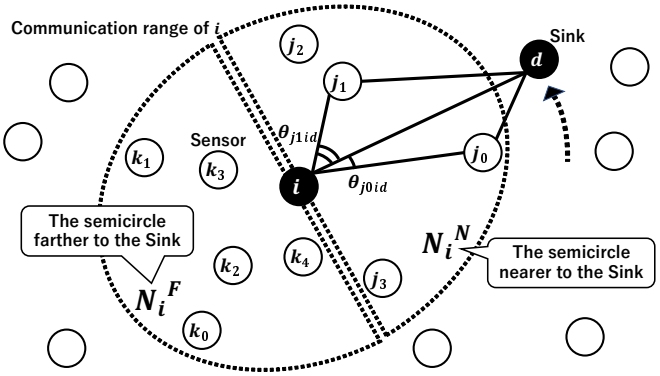

Fig. 2. Example of topology in P-bRS.

The results of computer simulation evaluations have confirmed that P-bRS improves the efficiency of the battery consumption and transmission delay of the nodes in comparison with the previous method. However, P-bRS does not consider the bandwidth utilization derived from the communications by other source nodes. Therefore, data collection may be difficult when congestion occurs in the area closest to the sink node if there are a lot of communications.

III. Adaptive Load Balancing Routing

In this paper, we propose a load balancing ad hoc routing, which can construct multiple paths based on transmission data size, available bandwidth of each link, and the residual battery of each node by applying PS to a dynamic network. We assume that the node can acquire maximum bandwidth and bandwidth utilization rate of all the links in the entire network.

Figure 3 shows the overview of PS in the proposed method. Here, the transmission data size between end-to-end nodes, transfer data size on each link and the transmission delay on each link in the figure correspond to the total amount of liquid, the flow rate of each tube and the length of each tube in physarum, respectively. Additionally, the bandwidth utilization rate is the rate occupied by the current usage bandwidth among the maximum bandwidth of a link. The bandwidth occupancy rate is the rate of the bandwidth occupied by the

transmission data size requested by the source node among the maximum bandwidth of the link. The bandwidth occupancy rate corresponds to the thickness of the tube in physarum.

Each node periodically calculates the bandwidth occupancy rate and the transmission delay time of all the links from the bandwidth utilization rate and the maximum bandwidth.

The operation procedure of the proposed method is shown below.

1) When a data transmission request occurs, the source node calculates the data packet transfer time $p_{ij}(t)$ by Eq. (7) and Eq. (8) from the transmission data size Q_{all}, bandwidth occupancy rate $D_{ij}(t)$, and the transmission delay $L_{ij}(t)$ between nodes i and j.

$$Q_{ij}(t) = \frac{D_{ij}(t)}{L_{ij}(t)} p_{ij}(t) \tag{7}$$

$$\sum_i Q_{ij} = \begin{cases} -Q_{\mathrm{all}} & (j = \mathrm{source}) \\ Q_{\mathrm{all}} & (j = \mathrm{destination}) \\ 0 & (\mathrm{otherwise}) \end{cases} \tag{8}$$

2) The source node calculates the transfer data size $Q_{ij}(t)$ on the link i–j from the data packet transfer time by Eq. (7). Consequently, a link that has a larger bandwidth occupancy rate and smaller transmission delay is allocated larger transfer data size.
3) The bandwidth occupancy rate is updated by Eq. (9).

$$D_{ij}(t+\delta t) = D_{ij}(t) + \delta t\{f(|Q_{ij}(t)|) - aD_{ij}(t)\} \tag{9}$$
$$Here, f(|Q_{ij}(t)|) = \frac{|Q_{ij}(t)|^{\mu}}{1+|Q_{ij}(t)|^{\mu}}, \quad \mu > 1.0$$

$\delta t\{f(|Q_{ij}(t)|) - aD_{ij}(t)\}$ in Eq. (9) represents the variation in the bandwidth occupancy rate after δt. The bandwidth occupancy rate asymptotically converges to specific values because the variation becomes small when using a sigmoid function, even if the transfer data size is large. Therefore, as the transmission data size increases, the number of links with saturated bandwidth occupancy rates also increase. The damping coefficient a in Eq. (9) is a parameter for changing the bandwidth occupancy rate independent of the transfer data size. It is normally set to 1. It enables a path to be constructed that prioritizes a relay node with a large amount of residual battery by changing the damping coefficient according to the residual battery of the node. Thereby, it may improve the route stability to avoid route disruption due to the loss of battery charge.

The source node iterates the above calculation until the transfer data size on each link converges. After convergence, the source node begins data packet transmission based on the transfer data size of each link, while distributing the traffic among the links. Therefore, the proposed method can transmit data along with a constructed route based on the transmission data size and available bandwidth.

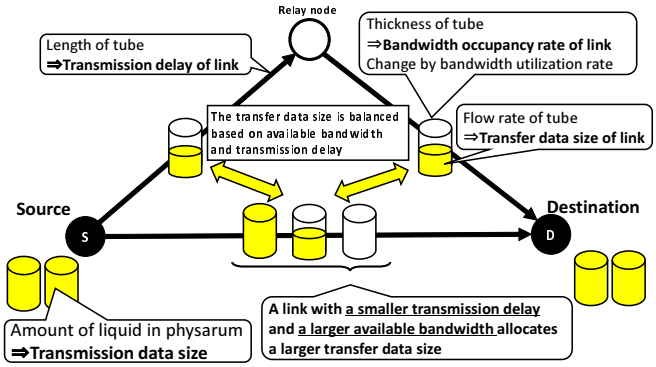

Fig. 3. The overview of PS in the proposed method.

IV. Performance Evaluation

A. Simulation Environment

The simulation evaluates the behavior and performance of the proposed method using proposed computer simulations. First, we made a simulation topology, as shown in Fig. 4. During the simulation, the maximum bandwidth of each link was set to 11 Mbps and the initial bandwidth utilization rate was set to 0%. We observed and evaluated the transition of the allocated transfer data size on each path as an evaluation index under several different conditions.

In this paper, we completed following simulations under different conditions.

1) ***Simulation 1:*** In simulation 1, we evaluate the effect of varying available bandwidth. We assume that the available bandwidth of each link is changed due to the radio interference in the simulation. Therefore, the maximum bandwidth of each link and bandwidth utilization rate of each link varies in the range between 1.0 and 11.0 Mbps and 1% to 100%, respectively, when the iteration count of calculations reaches 2,000 and 4,000 times. Figure 4 and Figure 5 show the simulation topology and available bandwidth on each link when the iteration count of calculations reaches 2,000 and 4,000 times.

2) ***Simulation 2:*** In simulation 2, we evaluate the effect of varying transmission data size. We assume the transmission data size is changed before determining a route. Therefore, the transmission data size is set to 5 MB at the initial time. Then, when the iteration count of calculations reaches 2,000 times, the transmission data size is changed to 10 MB, and when the iteration count of calculations reached 4,000 times, it changed to 5 MB.

3) ***Simulation 3:*** In simulation 3, we evaluate the effect of varying the residual battery of the node. In the topology of Fig. 4, node 3 transmits data packets with a higher frequency in comparison with other node because it is on the shortest path. Namely, the battery consumption of the node is also increased in comparison with the other node due to the above reason. Assuming that the node 3 excesses to consume its battery when the iteration count reaches 2,000 and 4,000 times, the damping coefficient of the link to node 3 adds one to the last value.

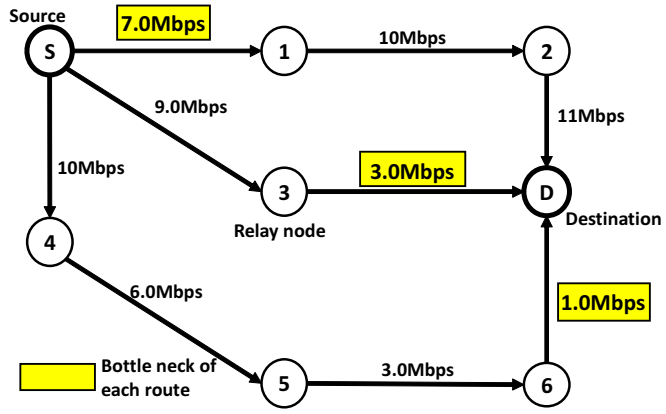

Fig. 4. Simulation topology and the available bandwidth when the iteration count is 2,000 (default is 11Mbps).

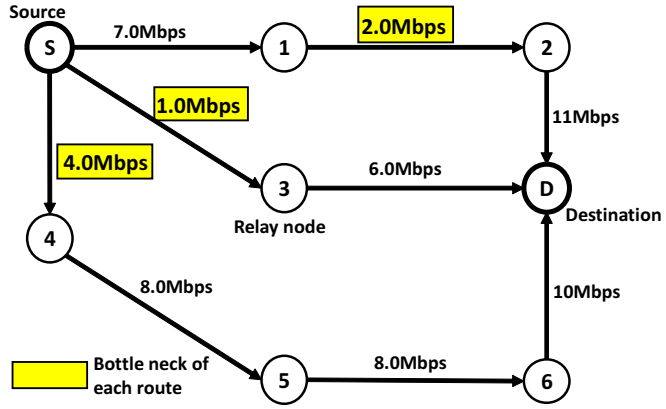

Fig. 5. Simulation topology and the available bandwidth when the iteration count is 4,000.

Additionally,, if the battery of node 3 increases and damping the link of bandwidth occupancy rate occurs, we expect the transfer frequency and the battery consumption of the nodes on the second shortest path S-1-2-D also increased. Thus, the damping coefficient of the link to node 1 adds one to every 1000 times after the iteration count reaches 6,000 times.

B. Evaluation Result

The results of the three simulations described in 4.1 are shown in Figures 6 to 8, Figure 9, and Figures 10 and 11, respectively. The simulations sufficiently iterate the calculation to observe the effect of convergence of the proposed method. Note that the iteration count can be shortened by aborting the calculation after a certain count, when the transfer data size is sufficiently converged in a practical situation.

1) ***Simulation 1:*** Figures 6 to 8, show that the transfer data size of the path is increases as the available bandwidth for each link increases. Furthermore, the transfer data size is distributed to the data packet transfer time to balance each utilization path. In particular, the path S-3-D with the minimum hop count is allocated the largest transfer data size among the paths at

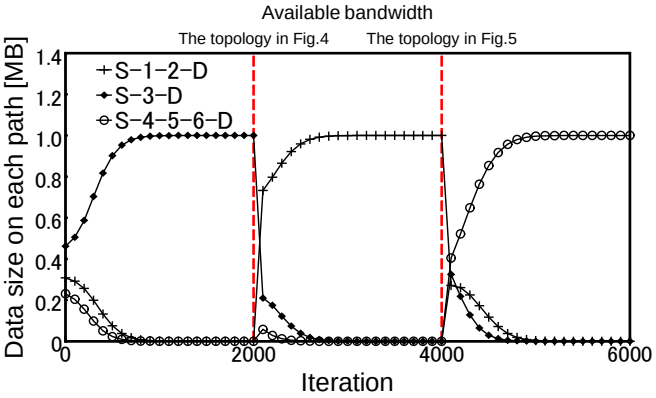

Fig. 6. Simulation 1: The transfer data size when the transmission data size is fixed to 1MB.

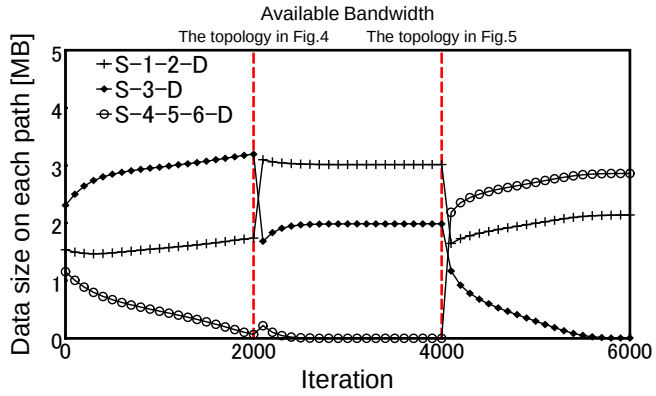

Fig. 7. Simulation 1: The transfer data size when the transmission data size is fixed to 5MB.

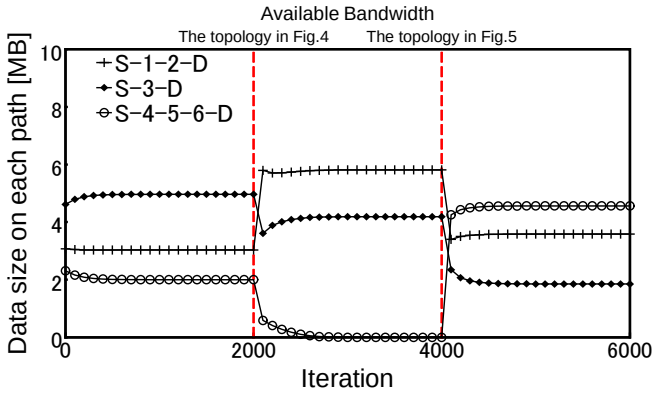

Fig. 8. Simulation 1: The transfer data size when the transmission data size is fixed to 10MB.

the initial state of the simulation. This is because the transfer data is preferentially allocated to the path with the minimum transmission delay because the available bandwidth of all links is uniform in the simulation.

2) ***Simulation 2:*** Figure 9 shows that the number of paths increased when the transmission data size increased. This is because the path S-4-5-6-D is constructed as the third path because the bandwidth occupancy rate of the other two paths is saturated owing to the increase of the transmission data size.

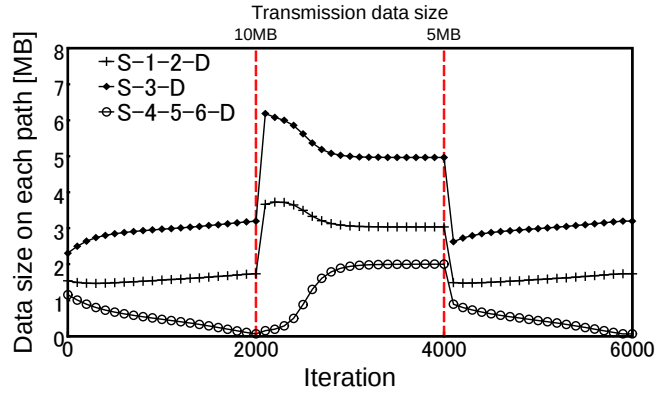

Fig. 9. Simulation 2: The transfer data size when varying transmission data size.

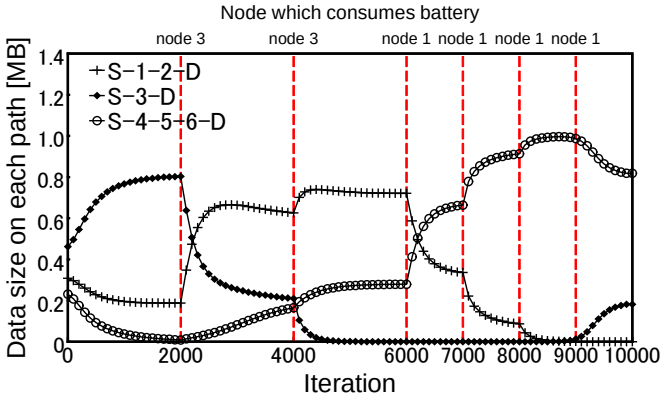

Fig. 10. Simulation 3: The transfer data size when varying residual battery (transmission data size :1MB).

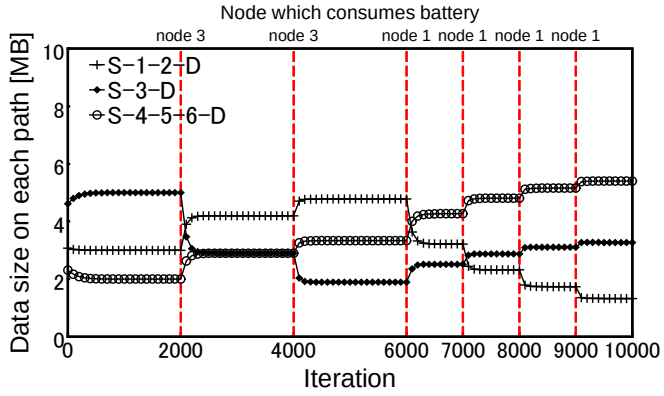

Fig. 11. Simulation 3: The transfer data size when varying residual battery (transmission data size :10MB).

Additionally, after the transmission data size is reduced to 5 MB, allocated transfer data size is also decreased and then the path S-4-5-6-D disappears. This is because the bandwidth occupancy rate of the other two paths gives a bandwidth margin due to a decrease in the transmission data size.

*3) **Simulation 3:*** Figure 10 shows that the detour path S-1-2-D is used because the transfer data size on the path S-3-D via node 3 decreases. The transfer data size on path S-4-5-6-D also increases. After, the transfer data size on path S-1-2-D decreases because node 1 consumes its battery, when the iteration count is 6,000 times. Finally, path S-4-5-6-D, that has a large amount of residual battery of the nodes, is used. Figure 11, shows that paths S-1-2-D and S-3-D do not disappear, unlike the result in Fig. 10. This is because the bandwidth occupancy rate of each path is saturated due to a large data size, and the variation of the transfer data size becomes very small. These results indicate that PS can select routes with a low risk of route disruption due to battery loss.

V. Conclusion

In this paper, we proposed an adaptive ad hoc routing method that can construct multiple paths based on the available bandwidth of each link, transmission data size, and residual battery of the node by applying PS to the dynamic networks. As a result of our simulations, we confirmed that the proposed method can adaptively construct single or multiple paths based on available bandwidth, transmission data size, and residual battery of nodes, in the dynamic network topology. In future, the increase in transmission delay due to the increasing of hop counts will be investigated. Additionally, we will conduct a detailed performance evaluation of the proposed method by extension of the existing routing protocol through a network simulator. Furthermore, the proposed method can be extended to be used in a table-driven routing protocol because the operation of the proposed method requires network information, such as the maximum bandwidth of the link.

Acknowledgment

This work was supported by JSPS KAKENHI Grant Number 17K12680.

References

[1] T. Nakagaki, H. Yamada, and A. Tóth, “Path finding by true morphogenesis in an amoeboid organism,” Biophys. Chem., vol. 92, pp. 47–52, Aug. 2001.

[2] G.-D. Caro, F. Ducatelle and L.-M. Gambardella, “AntHocNet: An adaptive nature-inspired algorithm for routing in mobile ad hoc networks,” Euro. Trans. Telecomms., vol. 16, pp. 443-”455, Sep. 2005.

[3] R. Leidenfrost and W. Elmenreich, “Firefly clock synchronization in an 802.15.4 wireless network,” EURASIP J. Embed. Syst., vol. 2009, pp. 1–17, Jan. 2009.

[4] S. Corson and J. Macker, “Mobile ad hoc networking (MANET): routing protocol performance issues and evaluation considerations,” IETF, RFC 2501, Jan. 1999.

[5] A. Tero, R. Kobayashi, and T. Nakagaki, “A mathematical model for adaptive transport network in path finding by true slime mold,” J. Theor. Biol., vol. 244, pp. 553–564, Feb. 2007.

[6] A. Tero, S. Takagi, and T. Saigusa, et al., “Rules for biologically inspired adaptive network design,” Science., vol. 327, pp. 439–442, Jan. 2010.

[7] A. Tero, R. Kobayashi, and T. Nakagaki, “Physarum solver: a biologically inspired method of road-network navigation,” Physica A., vol. 363, pp. 115–119, Apr. 2006.

[8] M. Zhang, W. Wei, R. Zheng, and Q. Wu, “P-bRS: A physarum-based routing scheme for wireless sensor networks,” Sci. World J., PMC 3932816, Feb. 2014.